



Performance enhancement in dye-sensitized solar cells by utilization of a bifunctional layer consisting of core–shell β -NaYF₄:Er³⁺/Yb³⁺@SiO₂ submicron hexagonal prisms

Kaimo Guo, Meiya Li*, Xiaoli Fang, Mengdai Luoshan, Lihua Bai, Xingzhong Zhao

School of Physics and Technology, and the Key Laboratory of Artificial Micro/Nano Structures of Ministry of Education, Wuhan University, Wuhan 430072, PR China

HIGHLIGHTS

- Synthesis of highly uniform β -NaYF₄:Er³⁺/Yb³⁺@SiO₂ core–shell hexagonal nano-prisms.
- Fabrication of DSSCs with β -NaYF₄:Er³⁺/Yb³⁺@SiO₂ as a bifunctional material.
- Enhanced light scattering and up-conversion were obtained in β -NaYF₄:Er³⁺/Yb³⁺@SiO₂.
- The properties of the DSSC with 15 wt % β -NaYF₄:Er³⁺/Yb³⁺@SiO₂ were greatly improved.
- Improvement is attributed to light scattering and up-conversion of β -NaYF₄:Er³⁺/Yb³⁺.

ARTICLE INFO

Article history:

Received 11 August 2013

Received in revised form

1 October 2013

Accepted 17 October 2013

Available online 25 October 2013

Keywords:

Silicon dioxide coated sodium yttrium fluoride core–shell structure

Light scattering

Up-conversion

DSSCs

Short-circuit current

Photoelectric conversion efficiency

ABSTRACT

Highly uniform, monodisperse β -NaYF₄:Yb³⁺/Er³⁺(NYFYE) up-conversion phosphor submicron hexagonal prisms coated with a SiO₂ layer are synthesized via a hydrothermal route, forming a core–shell NYFYE@SiO₂ crystallites. These crystallites are incorporated into TiO₂ nanocrystalline porous film to act as a bifunctional layer and form a composite photoanode employed in dye-sensitized solar cells (DSSCs). The influences of different amount of the NYFYE@SiO₂ on the performance of the composite photoanodes and DSSCs are investigated. Studies indicate that by adding NYFYE@SiO₂ the light scattering, absorption and near-infrared light harvesting of the composite photoanode are significantly increased, resulting in the great enhancement in the short-circuit current density (J_{sc}) and photoelectric conversion efficiency (η) of the DSSCs. The optimal properties with an J_{sc} of 14.91 mA cm⁻² and η of 7.28% are obtained in a DSSC with NYFYE@SiO₂ content of 15 wt %, increasing significantly by 14% and 29%, respectively, in comparison with those of the DSSC with pure TiO₂ photoanode. This significant enhancement in the performance of the DSSCs can be attributed to the enhanced light absorption due to the enhanced light scattering and near-infrared up-conversion of the NYFYE@SiO₂ bifunctional layer in the photoanode of the DSSCs.

© 2013 Elsevier B.V. All rights reserved.

1. Introduction

Exploitation and utilization of renewable energy has recently been proposed as a main solution for fossil fuel crisis and global warming. Among the candidates for the renewable energy so far, solar cell is a good choice. Dye-sensitized solar cells (DSSCs), first demonstrated by Oregan and Grätzel in 1991 [1], has been regarded as the most promising solar cells in the renewable

energy field due to its relatively high photoelectric conversion efficiency, potentially low cost and simple fabrication methodology [2–5]. Typically, a standard DSSC comprises a photoanode of dye-sensitized porous nanocrystalline TiO₂ film, a Pt-coated conductive glass as counter electrode and an electrolyte solution with a redox couple iodide/triiodide (I^-/I_3^-) between the electrodes. In order to improve the photoelectric conversion efficiency of DSSCs, various techniques, such as controlling TiO₂ photoanode into various nanostructural morphologies [6–8], dopants [9–11], new synthesized redox shuttles [12,13] and dyes capable of effectively absorbing visible and near-infrared light [14], have been explored. The dye adsorbed onto the surface of the porous TiO₂

* Corresponding author.

E-mail address: myli@whu.edu.cn (M. Li).

film of DSSCs plays an important role in harvesting sunlight. Upon light irradiation, the dye is promoted into an electronically excited state by absorbing photon and produce photo-stimulated electrons, and this electrons can transfer into the conduction band of the TiO_2 film. Thus, the light-harvesting efficiency (LHE) of the dye and the quantity of the photo-stimulated electrons would determine the efficiency of DSSCs to a great extent [15]. And enhancing the LHE of dye would be an effective way to increase the photoelectric conversion efficiency of DSSCs. However, the Ru dyes (N_3 and its derivatives), currently the most common used dyes in DSSCs, usually absorb light only up to about 700 nm due to their relatively large optical bandgap ($E_g = \sim 1.8 \text{ eV}$) [16], which means that approximately 50% energy of the solar spectrum in near-infrared (NIR) region is not utilized [16,17]. Consequently, the photoelectric conversion efficiency of DSSCs, to great extent, is limited by this spectral mismatch losses. Accordingly, extending the spectral response range of the photoanode to the NIR region is greatly expected to increase the photoelectric conversion efficiency of DSSCs.

Up-conversion (UC), first proposed in 1959 [18], refers to a nonlinear optical process in which an UC material can convert NIR light ($>900 \text{ nm}$) to visible light ($\leq 700 \text{ nm}$) by absorbing NIR low-energy photons and then emitting visible high-energy photons (anti-Stokes type emission). UC materials have recently received considerable attention due to their wide applications in biomedical imaging [19,20], semiconductor quantum dots and organic dyes [21], photovoltaic applications [22,23] and flat-panel displays monitors [24]. Among the investigated UC materials so far, the hexagonal phase(β -) of NaYF_4 host lattice doped with lanthanide combinations of $\text{Yb}^{3+}/\text{Er}^{3+}$ has the highest UC efficiency [25]. This $\beta\text{-NaYF}_4\text{:Yb}^{3+}/\text{Er}^{3+}$ (named as NYFYE) can generate strong green emission after absorbing NIR light [26]. Recently, studies on enhancing the photoelectric conversion efficiency of DSSCs via incorporating with such UC materials has been conducted [27,28]. For the purpose of matching well with nanocrystalline TiO_2 and light scattering demand, the crystallite size of the UC material used in the photoanode of DSSCs should be submicron or smaller. However, compared with bulk UC material, small UC crystallites show a classical drawback, namely poor luminescent efficiency. For example, in the case of lanthanide-based UC nano-crystallite, the presence of surface defects and ligands with high-energy vibrational modes such as OH or NH_2 groups can lead to the quenching of the excited lanthanide states by multiphonon relaxation processes (namely energy losses) [29,30]. In addition, the surface defects and ligands of the UC nano-crystallite in TiO_2 photoanode film would act as an electron trapping center and lead to charge recombination at the surface, which is the major limitation for their application in DSSCs [27]. Fortunately, coating UC nano-crystallite with an insulating layer to form a core–shell architecture helps to overcome this problem to some extent [28]. Therefore, by using the insulating SiO_2 as a coating layer to solve the above mentioned problem and prepare the core(NYFYE)-shell(SiO_2) structure (NYFYE@ SiO_2) crystallites and apply them in DSSCs, greatly enhancing the photoelectric conversion efficiency of DSSCs might be expected. However, such study has rarely been reported.

In this paper, we report the preparation of highly uniform and monodisperse core–shell structural NYFYE@ SiO_2 crystallites by hydrothermal method. Different amounts of NYFYE@ SiO_2 were incorporated into TiO_2 nanocrystalline films to form the composite photoanodes and then the DSSCs, as shown schematically in Fig. 1. The influence and mechanism of such NYFYE@ SiO_2 crystallites on the performance of the photoanodes and the DSSCs were investigated.

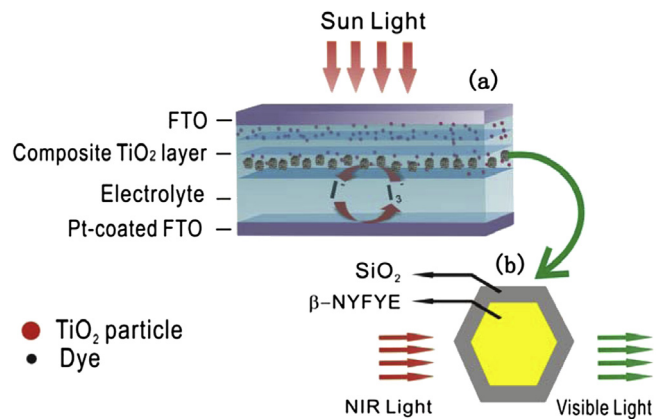


Fig. 1. (a) Schematic structure of the DSSCs incorporated with core–shell NYFYE@ SiO_2 in TiO_2 film. (b) Cross section of an NYFYE@ SiO_2 hexagonal prism and the schematic of the UC process.

2. Experimental section

2.1. Materials

NaF , $\text{Y}(\text{NO}_3)_3 \cdot 6\text{H}_2\text{O}$, $\text{Yb}(\text{NO}_3)_3 \cdot 6\text{H}_2\text{O}$ and $\text{Er}(\text{NO}_3)_3 \cdot 6\text{H}_2\text{O}$ were purchased from Wuhan Chemical Corporation (China). The ethanol (EtOH, 95%), Triton-X100, acetylacetone, Poly (ethylene glycol) (PEG, MW = 20,000), Tetraethylorthosilicate (TEOS, 99.9%), ammonia (28–30 wt % NH_3 in water), nitric acid (HNO_3 , 65% ~ 68%), polyvinylpyrrolidone (PVP, $M_w = 55 \text{ k}$ in terms of monomeric units) (>99.5%) and propylene carbonate (PC) were obtained from Sinopharm Chemical Reagent Corporation (China). The Ru dye and cis-di(thiocyanato)-bis(2,2'-bipyridyl-4,4'-dicarboxylate) ruthenium(II) (N719) were purchased from Solaronix (Switzerland). The Iodine (I_2 , 99.8%) was acquired from Beijing Yili Chemicals (China). Lithium iodide (LiI , 99%) and 4-tert-butylpyridine (TBP) were purchased from Acros (China). The fluorine-doped SnO_2 conductive glasses (FTO, sheet resistance $10\text{--}15 \Omega \text{ sq}^{-1}$, Asahi Glass, Japan) were used as the substrate for the preparation of mesoporous nanocrystalline TiO_2 film. All water used in the fabrication was deionized (18.2 M Ω , milli-Q pore).

2.2. Synthesis of NYFYE@ SiO_2 core–shell structure

NYFYE@ SiO_2 submicron hexagonal prisms with highly uniformity and monodispersity were grown by a modified hydrothermal reduction technique [31]. Typically, a DI-water solution (20 ml) in beaker containing $\text{Y}(\text{NO}_3)_3 \cdot 6\text{H}_2\text{O}$, $\text{Yb}(\text{NO}_3)_3 \cdot 6\text{H}_2\text{O}$ and $\text{Er}(\text{NO}_3)_3 \cdot 6\text{H}_2\text{O}$ (ion molar ratio, $\text{Y}/\text{Yb}/\text{Er} = 78:20:2$) were first prepared and stirred magnetically for 20 min; Then an aqueous solution of sodium citrate (40 ml) was added into the above solution, keeping for continuous stirring for 1 h. Subsequently, an aqueous solution (82 ml) of NaF (2.1 g) was added to the above solution and stirred for another 40 min. Finally, the pH value of the solution was adjusted to 3.5. Then the solution was transferred into two Teflon-lined autoclaves (100 ml for each) and heated at 200 °C for 4 h to obtain the submicron hexagonal prisms. This as-prepared NYFYE solution was then centrifuged at 6000 rpm for 5 min for three times and dried at 80 °C for 3 h to remove excess sodium citrate and obtain the white precipitates (NYFYE submicron hexagonal prisms). The white precipitates were then re-dispersed into EtOH solution and then coated with silica to form NYFYE@ SiO_2 core–shell structure by the modified Stober method [32]. The as-prepared NYFYE@ SiO_2 white powders were then collected by centrifugation and then dried at 80 °C for 3 h for further usage.

2.3. Fabrication of the photoanodes and DSSCs

The TiO_2 pastes were produced by ball milling TiO_2 powder [33]. The TiO_2 pastes containing different amounts of NYFYE@ SiO_2 were prepared according to a series of mass ratio (NYFYE: TiO_2 = 0, 5%, 10%, 15%, 20%). These pastes were coated on FTO glasses by doctor-blading technique, then dried under ambient conditions and sintered at 500 °C to obtain the photoanodes. Then, these photoanodes were dye-sensitized by immersing them into the solution of cis-di(thiocyanato)-bis(2,2'-bipyridyl-4,4'-dicarboxylate) ruthenium(II) (N719) with a concentration of 500 μM in the mixture of EtOH and tert-butyl alcohol (volume ratio: 1/1) at 60 °C overnight. Then these sensitized photoanodes were washed with EtOH to remove the dye molecules physisorbed on the surface of the nanocrystalline TiO_2 films to ensure that these films were covered with a monolayer of dye molecules and then dried in the oven at 60 °C. These photoanodes and the platinized counter electrodes were then assembled to form a series of DSSCs by sandwiching redox (I^-/I_3^-) electrolyte solution in between.

2.4. Characterizations

The morphologies of the NYFYE and NYFYE@ SiO_2 were characterized by a field-emission scanning electron microscope (SEM, JEOL, 6700F, Japan). The crystalline structures of these materials were determined by X-ray diffraction (XRD, D8 Advance, Bruker, Germany). High magnification images of the NYFYE prisms with and without SiO_2 coating were obtained by transmission electron microscope (TEM, JEM-2010FEF(UHR)) characterization. Moreover, the chemical species of the NYFYE@ SiO_2 were analyzed by Energy-dispersive X-ray spectroscopy (EDX, GENESIS 70000). The UV-vis absorption spectra of these samples were obtained on a UV-vis-NIR spectrophotometer (Cary 5000, Varian). The current density–voltage ($J-V$) characteristics of the DSSCs were measured under an irradiance of 100 mW cm^{-2} (AM 1.5 simulated illumination (Newport, 91192, Global)) and an effective

irradiating area of 0.25 cm^2 . Electrochemical impedance spectra (EIS) were recorded by a computer-controlled electrochemical workstation (CHI660C, Shanghai, China) in the condition of open circuit under 100 mW cm^{-2} irradiation and a frequency range of 100 kHz to 0.1 Hz. The amount of dye loaded on the photoanodes was measured by the UV-vis absorption spectra of the dye desorbed from these photoanodes by immersing them in a mixed solution of water and ethanol (volume ratio = 1:1) containing 0.1 M NaOH.

3. Results and discussion

3.1. Characterization of the NYFYE

Fig. 2a–c displays the typical SEM images of the NYFYE sample. A low magnification SEM image (Fig. 2a) shows that the as-synthesized sample consists of a large quantity of hexagonal submicron prisms with high uniformity, monodispersity, and well-defined crystallographic facets. Measurement statistically shows that these submicron prisms have an average size of about 483 nm in diameter and 422 nm in height. Moreover, from the SEM images of a higher magnification (Fig. 2b), we can see that these NYFYE prisms exhibit smooth surface with clear sharp edge, whereas the surface of the core–shell NYFYE@ SiO_2 prisms becomes a little rough (Fig. 2c). In addition, as can be seen from the XRD patterns, all the diffraction peaks seen in Fig. 2d can be well indexed to the data of the standard card of β -NaYF₄ (JCPDS file No.16-0334), suggesting that this sample consist of pure NYFYE crystals and that $\text{Yb}^{3+}/\text{Er}^{3+}$ have been effectively doped into the host lattices of the β -NaYF₄. Due to the amorphous structure of SiO_2 shell, no SiO_2 diffraction peak was found in the XRD pattern of the NYFYE@ SiO_2 . Moreover, the high intensity of the diffraction peaks of both the NYFYE and NYFYE@ SiO_2 in the XRD patterns further demonstrates that these samples are well crystallized. This is benefit for UC, because high crystallinity generally means less traps and stronger luminescence [26].

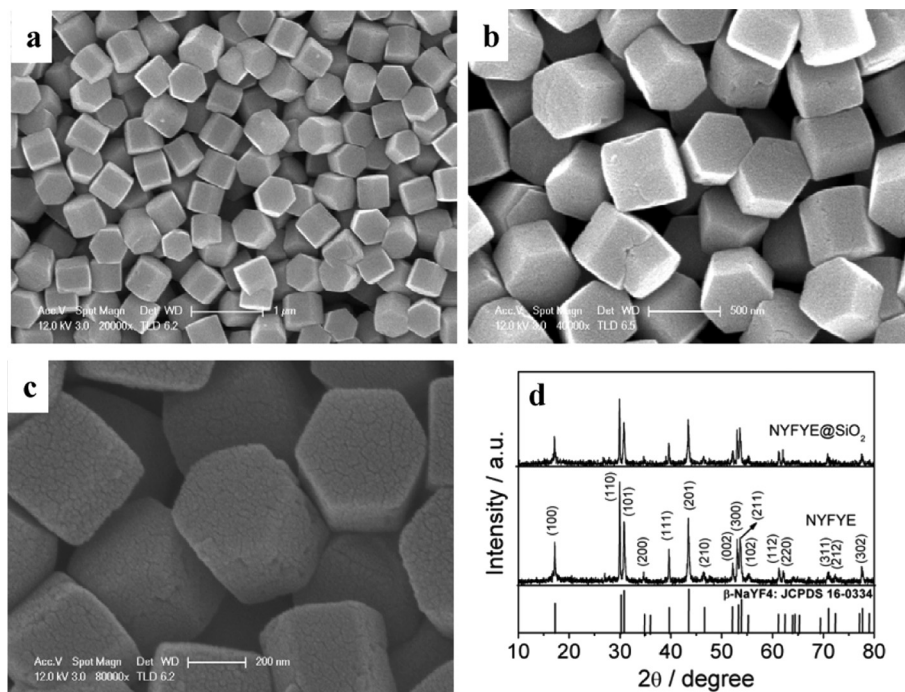


Fig. 2. Typical SEM images of the NYFYE at (a) lower magnification and (b) higher magnification; (c) SEM image of the NYFYE@ SiO_2 core–shell structure; (d) XRD patterns of the NYFYE and NYFYE@ SiO_2 .

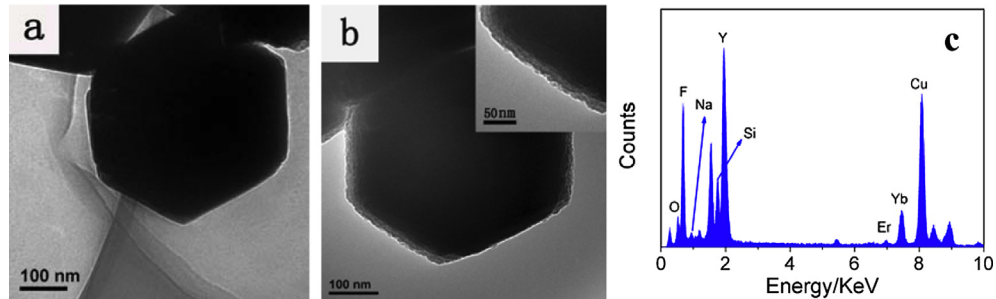


Fig. 3. TEM images of the NYFYE (a) and core–shell NYFYE@SiO₂ (b) submicron prisms; (c) EDS pattern of the core–shell NYFYE@SiO₂.

Fig. 3a–b shows TEM images of the NYFYE and NYFYE@SiO₂ prisms. In comparison with the bare NYFYE (Fig. 3a), it can be seen clearly that the whole NYFYE prism was coated well by a uniform SiO₂ shell, forming a core–shell NYFYE@SiO₂ structure (Fig. 3b). Further evidence for the core–shell structure of the NYFYE@SiO₂ was also obtained by the EDS spectrum (Fig. 3c), in which the peaks of Si and O were both observed.

3.2. Spectra characteristics of the NYFYE

Fig. 4a displays the absorption spectra of the NYFYE prisms in colloidal dispersion. An absorption peak at a wavelength of about 980 nm was clearly observed, which corresponds to the transition of the Yb³⁺ ions in between the energy level ²F_{7/2} to ²F_{5/2} [31]. As aforementioned, NYFYE@SiO₂, being an UC material, is capable of converting NIR to visible light, which can be confirmed by the fluorescence spectrum of the NYFYE@SiO₂. Under the excitation of 980 nm NIR light, two UC emission bands of the NYFYE@SiO₂ in the curve (see the blue line of Fig. 4a), centered at nearly 543 nm (green emission band A) and 655 nm (red emission band B) arised by two photon processes (see Fig. 4b), are observed, respectively [27]. The

green light corresponds to the emission from the excited states of Er³⁺ of ²H_{11/2}, ⁴F_{7/2}, and ⁴S_{3/2} to the ground state of ⁴I_{15/2}, and the red one results from the emission from the excited state ⁴F_{9/2} to the ground state ⁴I_{15/2} [30]. These visible lights converted from the NIR light can be effectively absorbed by the N719 dye as shown by its absorption spectra (Fig. 4c), which improve the utilization of incident light and then the efficiency of the DSSCs.

3.3. Influences of the NYFYE on the performance of the photoanode

In order to assess the effect of NYFYE@SiO₂ on the light response of the composite films, the UV–vis spectra of the composite films incorporated with different amounts of NYFYE@SiO₂ were measured and presented in Fig. 5. The light absorption of the composite films increases with the increase of the NYFYE@SiO₂ in the films in the whole visible region in comparison with that of the pure TiO₂ film, as shown in Fig. 5a. This notably enhancement in light absorption should be mainly attributed to the scattering effect of the NYFYE@SiO₂ in the films [27], which would reduce the transmission of the incident light, extend the optical path inside the films and thus increase the LHE [28]. To verify our above inference,

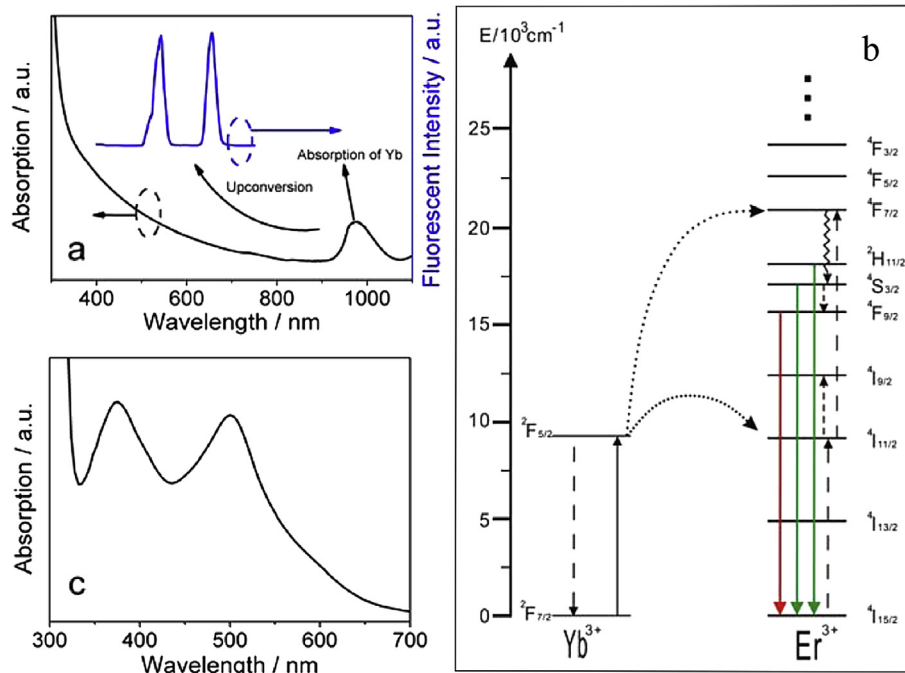


Fig. 4. (a) The UV–vis absorption (black line) and UC fluorescence (blue line) spectra of the NYFYE@SiO₂; (b) the diagrams of energy levels of Yb³⁺–Er³⁺ and UC luminescence processes in an Yb³⁺–Er³⁺ codoped system upon 980 nm excitation; (c) UV–vis absorption spectrum of the N719 dye. (For interpretation of the references to color in this figure legend, the reader is referred to the web version of this article.)

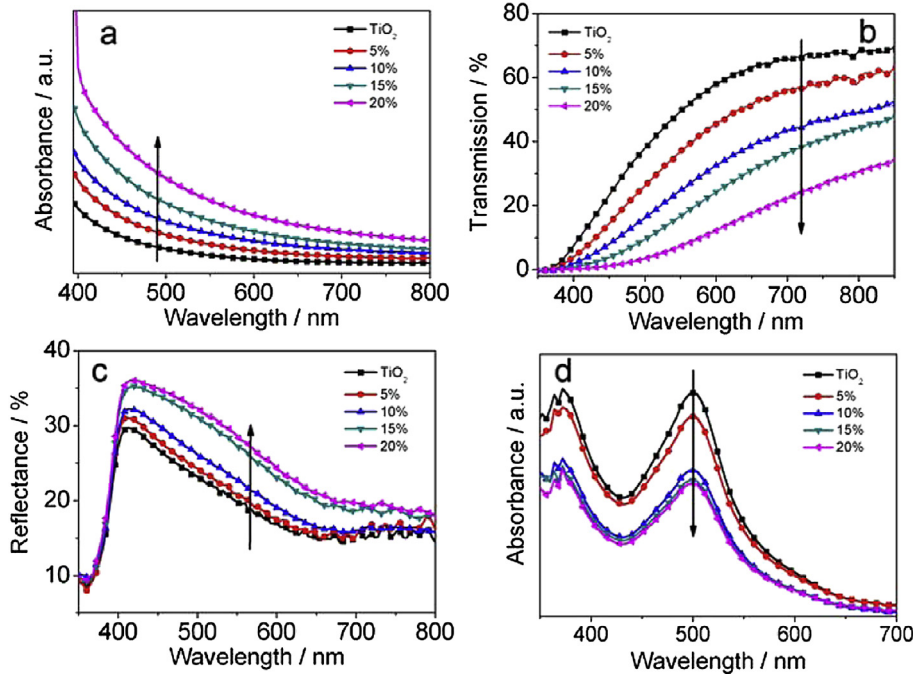


Fig. 5. UV-vis absorption spectra (a), transmittance spectra (b), and scattering spectra (c) of the TiO₂ films containing different amounts of NYFYE@SiO₂. (d) UV-vis absorption spectra of the dyes desorbed from the TiO₂ films with different amounts of NYFYE@SiO₂.

both of the transmittance (Fig. 5b) and scattering (Fig. 5c) spectra of these films were measured. As one can see in Fig. 5b, the light transmission of the composite films decrease and the light scattering (reflection) of the films increase, respectively, with the increase of the added NYFYE@SiO₂ (Fig. 5c), suggesting that the NYFYE@SiO₂ acts as scattering center and increases light path inside the mesoporous photoanode. To further confirm above result, the amount of dyes loaded onto each film were measured. The UV-vis absorption spectra of the dye desorbed from the dye-sensitized TiO₂ films measured in NaOH solution are shown in Fig. 5d. It is noted that the intensity of the absorption peak at around 500 nm of the dye desorbed from the TiO₂ films with NYFYE@SiO₂ is slightly lower than that of the pure TiO₂ film, indicating that the amount of dye loaded in the TiO₂ films containing NYFYE@SiO₂ decreases. This decrease in amount of the adsorbed dye might be the result of the possible decreased surface area of the TiO₂ porous films due to the incorporation of the NYFYE@SiO₂. In spite of the less amount of dye loaded in the TiO₂ films with NYFYE@SiO₂, these films have stronger light absorption than that of the pure TiO₂ film, which confirms our aforementioned inference that the enhanced light absorption of these composite TiO₂ films is not arisen from the

increase of dye but the enhanced light scattering inside the photoanode film arising from NYFYE@SiO₂ crystallites.

3.4. Effects of NYFYE on the performance of DSSCs

To investigate the effects of the core-shell NYFYE@SiO₂ particles on the performance of DSSCs, a serial of DSSCs made of N719-sensitized TiO₂ film photoanodes with different contents of the core-shell NYFYE@SiO₂ particles were prepared. For comparison purpose, the DSSC based on pure TiO₂ photoanode was also prepared. Fig. 6a shows the photocurrent density–voltage (*J*–*V*) characteristics of these DSSCs, and their performance parameters are tabulated in Table 1. Fig. 6b presents the dependence of the performance parameters (*J*_{sc}, η) of the DSSCs on the amount of NYFYE@SiO₂ in the TiO₂ films. As can be seen from Fig. 6b, both *J*_{sc} and η exhibit an increase and then decrease changes with the increasing concentration of NYFYE@SiO₂. For the DSSC containing 15 wt % of the NYFYE@SiO₂, the optimized performance with a *J*_{sc} of 14.19 mA cm⁻², *V*_{oc} of 766 mV and η of 7.28% is achieved, exhibiting a ~14%, ~5% and ~29% enhancement respectively in comparison with those of the DSSC with pure TiO₂ photoanode. These

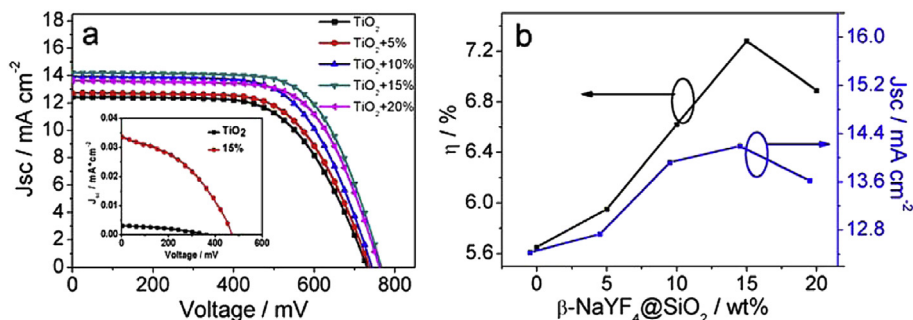


Fig. 6. (a) *J*–*V* curves of the DSSCs as a function of the concentration of NYFYE@SiO₂ (the inset is the *J*–*V* curve of the DSSCs with 0 wt % and 15 wt % NYFYE@SiO₂ addition at 980 nm NIR light irradiation); (b) *J*_{sc} and η of the DSSCs varying with the concentration of NYFYE@SiO₂.

Table 1

Performance parameters of the DSSCs varying with different contents of NYFYE@SiO₂.

Group	$J_{sc}/\text{mA cm}^{-2}$	V_{oc}/mV	FF	$\eta/\%$	R_2/Ω	Dye amount/ $\times 10^{-7} \text{ mol cm}^{-2}$
TiO ₂	12.43	731	0.62	5.65	12.8	1.364
5 wt %	12.73	737	0.63	5.95	19.1	1.214
10 wt %	13.93	742	0.64	6.62	19.8	1.186
15 wt %	14.19	766	0.66	7.28	22.6	1.147
20 wt %	13.62	761	0.66	6.89	24.3	1.132

improvements in performance are consistent with the UV–vis spectra (Fig. 5a–c). As aforementioned, the amount of dye loaded in the TiO₂ films with NYFYE@SiO₂ is a little less than that of the pure TiO₂ film (Fig. 5d). Therefore, the increases in J_{sc} and η could be mainly attributed to the scattering effect [Fig. 5c] and the UC function of the NYFYE@SiO₂ [27,34]. To confirm the UC function, the photovoltaic response (inset of Fig. 6a) of the optimized DSSC with 15 wt % NYFYE@SiO₂ addition was also measured under illumination of NIR light source of 980 nm (0.4 W power) and the irradiated area of about 0.2 cm² 469 mV of V_{oc} and 0.033 mA cm⁻² of J_{sc} were obtained in the DSSC, which are superior than that of the DSSC with pure TiO₂ film and are similar with those reported [28]. This result combined with that shown in Fig. 4b confirm that the improvement of the DSSC performance is also due to the UC of the NYFYE@SiO₂.

However, with further increasing the amount of NYFYE@SiO₂ over 15 wt %, the J_{sc} decreases accordingly (see Table 1 and Fig. 6). One reason for this decrease in J_{sc} can be associated with the excess amount of NYFYE@SiO₂ in TiO₂ films that may reduce the effective surface area of TiO₂ films and the amount of dye absorbed (Fig. 5d) [35]; Therefore, when the increase of the photocurrent resulted from the scattering and UC of the NYFYE@SiO₂ crystallites is not enough to compensate the decrease of the photocurrent resulted from the decrease of the absorbed dye due to the NYFYE@SiO₂ addition, the continued increase of the NYFYE@SiO₂ would result in the decrease of J_{sc} . Another reason for the decrease in J_{sc} might be associated with the insulating property of these NYFYE@SiO₂ crystallites embedded in the TiO₂ matrix. Due to the insulating property of these NYFYE@SiO₂, the connection between the semiconductor TiO₂ nanoparticles was obstructed. This suggests that some photogenerated electrons have to get around these nonconductor NYFYE@SiO₂ crystallites and then reach to the collecting electrode. Therefore, the transporting path of electrons is prolonged, and then the recombination possibility of the electrons at the interface of dye/TiO₂/electrolyte increases [27], resulting in the decrease in J_{sc} to some extent when the content of NYFYE@SiO₂ exceeding 15%.

To get further insight into the difference in the charge transfer resistance at the interfaces of the conducting layer/TiO₂, Pt/electrolyte, and dye/TiO₂/electrolyte in DSSCs, the EIS of the DSSCs were measured [36]. Fig. 7 shows the typical EIS Nyquist plots of the DSSCs with different amount of NYFYE@SiO₂. From left to right in the figure, the R_s is the sheet resistance of the FTO layer, the first semicircle Z_1 represents the complex impedance of the charge transfer at the TiO₂ conduction layer or the counter-electrode-Pt/electrolyte interfaces, and the second semicircle Z_2 stands for the complex impedance of the TiO₂/dye/electrolyte interface [37]. Due to the identical of the Pt-coated counter-electrodes and FTO glasses used in the DSSCs, the influences of Z_1 and R_s can be ignored. Therefore, our main concern, here, is focused on the TiO₂/dye/electrolyte interface transfer impedance Z_2 . It can be seen clearly from Fig. 7, with the increase of the NYFYE@SiO₂, the diameter of the Z_2 increase, i.e. the electron transfer resistance R_2 (real part of Z_2 , the diameter of the semicircle) of the TiO₂/dye/electrolyte interface increases. The R_2 derived from Z_2 by an equivalent circuit

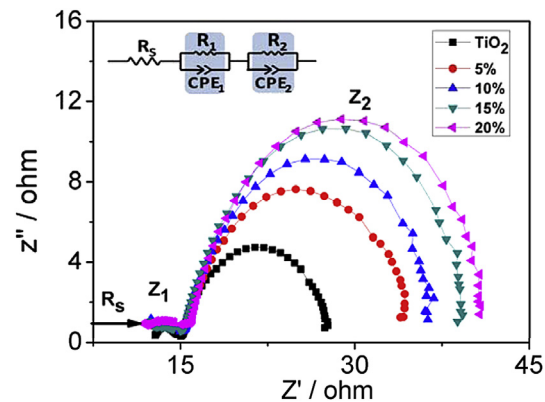


Fig. 7. The Nyquist plots of EIS for the DSSCs as a function of NYFYE@SiO₂ contents (inset is the equivalent circuit).

fitting (the inset of Fig. 7) are summarized in Table 1. As shown in Table 1, the R_2 increases from 12.8 Ω for the conventional DSSC to 24.3 Ω for the DSSC with 20 wt % NYFYE@SiO₂. As discussed before, the reason for the R_2 increased with the increase of the NYFYE@SiO₂ is that the non-conductive NYFYE@SiO₂ obstruct electron transfer in the TiO₂ porous film to some extent. The larger the R_2 , the more is the electron recombination at the dye/TiO₂/electrolyte interface [34], and the smaller is the J_{sc} . This also confirm that the adding of excess amount (20 wt %) of NYFYE@SiO₂ in TiO₂ films not only reduces the dye loading, but also obstructs the electron transfer, and these disadvantages compensates the improvements in properties of DSSCs due to the enhanced scattering and UC, and thus results in the decreased J_{sc} and η of the DSSCs (Fig. 6b).

4. Conclusions

In this work, novel up-conversion phosphor, core–shell NYFYE@SiO₂ submicron hexagonal prisms were successfully synthesized and incorporated into TiO₂ photoanode film acting as a bifunctional layer for DSSCs. The influences of different amount of NYFYE@SiO₂ on the performance of the photoanodes and DSSCs were investigated. Studies reveal that with the increase of the incorporated NYFYE@SiO₂, the light absorption and scattering of the complex photoanode in the visible region increase, while the transmission of incident light and the amount of dye absorbed in the photoanode decrease. The J_{sc} and η increase first and then decrease with the increase of the NYFYE@SiO₂. The optimal properties were obtained in a DSSC with an J_{sc} of 14.19 mA cm⁻² and η of 7.28% at the NYFYE@SiO₂ content of 15 wt %, about 14% and 29% superior to those of the DSSC with pure TiO₂ photoanode, respectively. This significant enhancement in the performance of the DSSCs can be attributed to the enhanced light absorption due to the enhanced light scattering and NIR up-conversion of the NYFYE@SiO₂ bifunctional layer in the photoanode of the DSSCs.

Acknowledgments

This work was supported by the National Basic Research Program of China (granted No. 2011CB93304) and the Fundamental Research Funds for the Central Universities (Granted No.: 20102020101000036).

References

- [1] B. Oregan, M. Grätzel, *Nature* 353 (1991) 737–740.
- [2] M. Grätzel, *Nature* 414 (2001) 338–344.

- [3] C.Y. Chen, M.K. Wang, J.Y. Li, N. Pootrakulchote, L. Alibabaei, C.H. Ngocle, J.D. Decoppe, J.H. Tsai, C. Grätzel, C.G. Wu, S.M. Zakeeruddin, M. Grätzel, *ACS Nano* 3 (2009) 3103–3109.
- [4] A. Yella, H.W. Lee, H.N. Tsao, C.Y. Yi, A.K. Chandiran, M.K. Nazeeruddin, E.W.G. Diau, C.Y. Yeh, S.M. Zakeeruddin, M. Grätzel, *Science* 334 (2011) 629–634.
- [5] F. Gong, H. Wang, X. Xu, G. Zhou, Z.S. Wang, *J. Am. Chem. Soc.* 134 (2012) 10953–10958.
- [6] M. Adachi, Y. Murata, J.T. Kao, J.T. Jiu, M. Sakamoto, F.M. Wang, *J. Am. Chem. Soc.* 126 (2004) 14943–14949.
- [7] L.H. Hu, S.Y. Dai, J. Weng, S.F. Xiao, Y.F. Sui, Y. Huang, S.H. Chen, F.T. Kong, X. Pan, L.Y. Liang, K.J. Wang, *J. Phys. Chem. B* 111 (2007) 358–362.
- [8] D.H. Chen, F.Z. Huang, Y.B. Cheng, R.A. Caruso, *Adv. Mater.* 21 (2009) 2206–2210.
- [9] T.L. Ma, M. Akiyama, E. Abe, I. Imai, *Nano Lett.* 5 (2005) 2543–2547.
- [10] H.J. Tian, L.H. Hu, W.X. Li, J. Sheng, S.Y. Xu, S.Y. Dai, *J. Mater. Chem.* 21 (2011) 7074–7077.
- [11] X.L. Fang, M.Y. Li, K.M. Guo, Y.D. Zhu, Z.Q. Hu, X.L. Liu, B.L. Chen, X.Z. Zhao, *Electrochim. Acta* 65 (2012) 174–178.
- [12] J.N. Clifford, E. Palomares, M.K. Nazeeruddin, R. Thampi, M. Grätzel, J.R. Durrant, *J. Am. Chem. Soc.* 126 (2004) 5670–5671.
- [13] C.Y. Lee, J.T. Hupp, *Langmuir* 26 (2010) 3760–3765.
- [14] T.C. Li, A.M. Spokoyny, C.X. She, O.K. Farha, C.A. Mirkin, T.J. Marks, J.T. Hupp, *J. Am. Chem. Soc.* 132 (2010) 4580–4582.
- [15] M. Grätzel, *Acc. Chem. Res.* 42 (2009) 1788–1798.
- [16] J.C.G. Bünzli, S.V. Eliseeva, *J. Rare Earths* 28 (2010) 824–842.
- [17] Q.F. Zhang, G.Z. Cao, *Nano Today* 6 (2011) 91–109.
- [18] N. Bloembergen, *Phys. Rev. Lett.* 2 (1959) 84–85.
- [19] L.Y. Wang, P. Li, Y.D. Li, *Adv. Mater.* 19 (2007) 3304–3307.
- [20] D.K. Chatterjee, A.J. Rufaihah, Y. Zhang, *Biomaterials* 29 (2008) 937–943.
- [21] C. Feldman, T. Justel, C.R. Ronda, P.J. Schmidt, *Adv. Funct. Mater.* 13 (2003) 511–516.
- [22] J.D. Wild, A. Meijerink, J.K. Rath, W.G.J.H.M. van Sark, R.E.I. Schropp, *Sol. Energy Mater. Sol. Cells* 94 (2010) 1919–1922.
- [23] H.Q. Wang, M. Batentschuk, A. Osvet, L. Pinna, C.J. Brabec, *Adv. Mater.* 23 (2011) 2675–2680.
- [24] A. Rapaport, J. Milliez, M. Bass, L. Fellow, A. Cassanho, *J. Disp. Technol.* 2 (2006) 68–78.
- [25] S. Heer, K. Kompe, H.U. Gudel, M. Haase, *Adv. Mater.* 16 (2004) 2102–2105.
- [26] C.X. Li, Z.W. Quan, J. Yang, P.P. Yang, J. Lin, *Inorg. Chem.* 46 (2007) 6329–6336.
- [27] G.B. Shan, G.P. Demopoulos, *Adv. Mater.* 22 (2010) 4373–4377.
- [28] G.B. Shan, H. Assaadoui, G.P. Demopoulos, *ACS Appl. Mater. Interfaces* 3 (2011) 3239–3243.
- [29] F. Wang, J. Wang, X. Liu, *Angew. Chem.* 122 (2010) 7618–7622.
- [30] M. Haase, H. Schäfer, *Angew. Chem. Int. Ed.* 50 (2011) 5808–5829.
- [31] F. Wang, Y. Han, C.S. Lim, Y.H. Lu, J. Wang, J. Xu, H.Y. Chen, C. Zhang, M.H. Hong, X.G. Liu, *Nature* 463 (2010) 1061–1065.
- [32] W. Stober, A. Fink, E. Bohn, *J. Colloid Interface Sci.* 26 (1968) 62–69.
- [33] K.M. Guo, M.Y. Li, X.L. Fang, X.L. Liu, B. Sebo, Y.D. Zhu, Z.Q. Hu, X.Z. Zhao, *J. Power Sources* 230 (2013) 155–160.
- [34] C. Hägglund, M. Zäck, B. Kasemo, *Appl. Phys. Lett.* 92 (2008) 013113–1–013113–3.
- [35] W.B. Hou, P. Pavaskar, Z.W. Liu, J. Theiss, M. Aykol, S.B. Cronin, *Energy Environ. Sci.* 4 (2011) 4650–4655.
- [36] Q. Wang, J.E. Moser, M. Grätzel, *J. Phys. Chem. B* 109 (2005) 14945–14953.
- [37] L.Y. Han, N. Koide, Y. Chiba, T. Mitate, *Appl. Phys. Lett.* 84 (2004) 2433–2435.